Optimized nonadiabatic nanofocusing of plasmons by tapered metal rods

Dmitri K. Gramotnev,[1,a)] Michael W. Vogel,[1] and Mark I. Stockman[2]

[1]*Applied Optics Program, School of Physical and Chemical Sciences, Queensland University of Technology,
G.P.O. Box 2434, Brisbane QLD 4001, Australia*
[2]*Department of Physics and Astronomy, Georgia State University, University Plaza,
Atlanta, Georgia 30303-3083, USA*

Using rigorous numerical methods of analysis, this paper investigates nonadiabatic nanofocusing in tapered nanorods with the major emphasis on structural optimization for achieving maximal possible local field enhancement. Simple analytical equations for the determination of the optimal length of the tapered rod are presented and discussed. It is also shown that for the considered structures, optimal taper angle and optimal length of the rod only very weakly depend on the radius of curvature of the rounded tip of the rod. Contrary to this, enhancement of the local electric field at the rounded tip strongly increases with decreasing radius of the tip. Comparison of the numerical results with the adiabatic theory of nanofocusing results in accurate verification of the applicability conditions for adiabatic approximation in tapered nanorods. © *2008 American Institute of Physics.*
[DOI: 10.1063/1.2963699]

I. INTRODUCTION

A major problem in modern nano-optics is related to effective concentration and delivery of electromagnetic energy to nanoscale regions.[1–22] This is especially important for imaging and diagnostics with nanoscale resolution (in near-field microscopy and spectroscopy), efficient coupling of light into and out of nano-optical interconnectors and devices, electromagnetic probing of separate molecules and quantum dots, nonlinear plasmonics, etc. One of the current resolutions of this problem is related to using plasmon nanofocusing in metal nanostructures.[1–22] These include dielectric conical tips covered with a metal film,[1–8] sharply tapered metal rods,[11–15] nanoparticle lenses,[9,10] sharp *V*-grooves, and nanowedges.[16–22]

Among the most promising structures for effective plasmon nanofocusing are sharply tapered metal nanorods.[11–15] This is because, when dissipation in the metal is relatively weak, nanorods typically provide significantly stronger local field enhancement compared to the other considered nanofocusing structures (when dissipation is strong, this may not always be the case[20]). The analysis of plasmon nanofocusing in metal rods has been based on the approximate solution of the wave equation[11] (though applicability conditions for this approach are fairly restrictive), adiabatic approximation,[12,13] and rigorous numerical analysis based on the finite-element approach (using the commercially available COMSOL software package).[14,15]

The recent paper by Issa and Guckenberger[14] has reported the results of the first rigorous numerical analysis of nonadiabatic plasmon nanofocusing in metal rods with rounded tips and arbitrary taper angles. These results include several important features one of which is the existence of an optimal taper angle for the rod (similar to that for tapered nanogaps[17,20]) for achieving strong local field enhancement at the tip.[14] The dependence of this optimal taper angle on wavelength has also been investigated, demonstrating a significant decrease in the optimal angle together with the simultaneous increase in the local field enhancement at the tip, when plasmon frequency is decreased.[14] It has also been shown that increasing the length of the tapered rod, while keeping the taper angle constant, also results in an increase in the local field enhancement at the tip (while the optimal taper angle does not seem to depend on the length of the nanofocusing rod).[14]

However, several important questions still remain unanswered. For example, no analysis of the local field enhancement as a function of the radius of the tip has been conducted so far. No comparison with the previously developed adiabatic theory of plasmon nanofocusing in tapered rods has been done, which leaves open the question about the actual applicability of the adiabatic theory at relatively large taper angles. Though it has been shown that increasing the length of the rod results in an increase in the local field enhancement at the tip, it is still not clear if this trend will continue for all rod lengths, or there is an optimal length at which the local field enhancement at the tip is maximal. All these questions are important for the practical applications of plasmon nanofocusing in tapered rods and optimal design of these structures.

Therefore, the aim of this paper is to conduct numerical optimization of tapered nanofocusing metal rods and to determine the optimal conditions and structural parameters for achieving maximal possible local field enhancement at the tip. In particular, it will be shown that there exists an optimal length of the tapered rod, and a simple analytical condition for an optimal geometry of the rod will be derived and discussed. Typical values of the maximal possible local field enhancement in practically realistic structures will also be determined. Detailed comparison of the numerical rigorous analysis of plasmon nanofocusing with the previously devel-

---

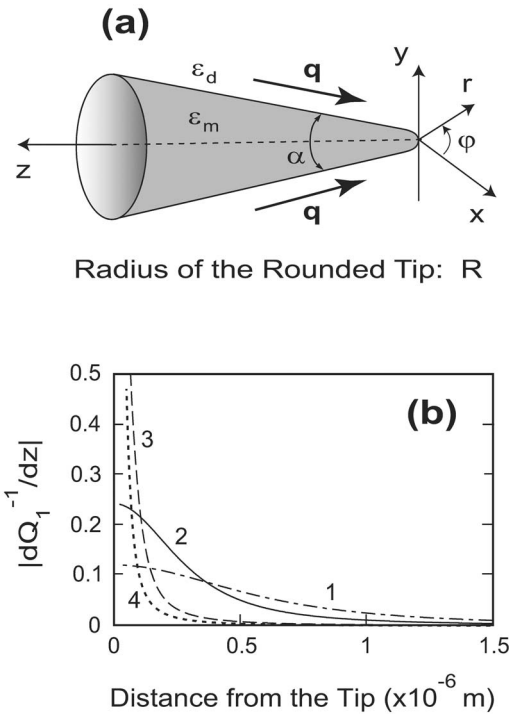a)Electronic mail: d.gramotnev@qut.edu.au.

(a)

Radius of the Rounded Tip: R

(b)

FIG. 1. (a) A metal rod with the taper angle α, permittivity $\varepsilon_m = e_1 + ie_2$, and rounded tip of radius R, surrounded by a lossless dielectric material with the real and positive permittivity ε_d, **q** is the wave vector of the TM surface plasmon propagating toward the tip of the rod, and (x, y, z) and (r, φ, z) are the Cartesian and cylindrical systems of coordinates. (b) The dependencies of the left-hand side of inequality (1) on the distance from the tip with $R = 0$ for the gold rods surrounded by vacuum at the vacuum wavelength $\lambda_{vac} = 632.8$ nm [$\varepsilon_m = -11.44 + 1.12i$ (Ref. 23) and $\varepsilon_d = 1$] and different taper angles: (1) $\alpha = 5°$, (2) $\alpha = 10°$, (3) $\alpha = 50°$, and (4) $\alpha = 90°$; Q_1 is the real part of the plasmon wave number q.

oped adiabatic theory[12,13] will be conducted, resulting in further validation of the applicability conditions for the adiabatic approximation.

II. STRUCTURE AND METHODS OF ANALYSIS

The analyzed structure is presented in Fig. 1(a). A tapered metallic rod with a taper angle α and complex permittivity $\varepsilon_m = e_1 + ie_2$ ($e_1 < 0$, $e_2 > 0$) is surrounded by a lossless dielectric medium with a permittivity ε_d (we will primarily limit our consideration to the case of the tip surrounded by vacuum, i.e., $\varepsilon_d = 1$). The coordinate axes are shown in Fig. 1(a). The analysis will be conducted for the plasmon mode of TM polarization with both the electric and magnetic fields independent of the angle φ, and magnetic field parallel to the φ-axis. This is because only such TM plasmons can exist at arbitrarily small rod diameters and thus experience nanofocusing in a tapered rod.[12,13]

If the taper angle of the rod is sufficiently small, so that the variations of the plasmon wave number within one plasmon wavelength are negligible at all distances from the tip of the rod, then the adiabatic (geometrical optics) approximation can be used for the analysis of nanofocusing. Mathematically, the applicability condition for the adiabatic approximation can be written as[12,13,16,18,20,21]

$$\left| \frac{d(Q_1)^{-1}}{dz} \right| \ll 1, \tag{1}$$

where Q_1 is the real part of the plasmon wave number $q = Q_1 + iQ_2$, and plasmon dissipation is assumed to be weak: $Q_2 \ll Q_1$.

Figure 1(b) presents the dependencies of the left-hand side of inequality (1) on the distance from the tip of the gold rod in vacuum with the radius of curvature of the tip $R = 0$ for the vacuum wavelength $\lambda_{vac} = 632.8$ nm [$\varepsilon_m = -11.44 + 1.12i$ (Ref. 23) and $\varepsilon_d = 1$] and different taper angles. In particular, it can be seen that if the taper angle is increased, then inequality (1) may be breached near the tip [curves 3 and 4 in Fig. 1(b)], while sufficiently far from the tip, where the rod diameter is larger than the plasmon wavelength, it is satisfied at all taper angles [Fig. 1(b)]. This is because the plasmon wave number starts to vary significantly (at large α) with reducing rod diameter only when this diameter becomes smaller than the plasmon wavelength. Therefore, the adiabatic approximation can be used for the analysis of plasmon propagation sufficiently far from the tip of the rod practically at all taper angles. This is only near the tip, where condition (1) imposes significant restrictions on the taper angle.

As a result, in this paper, we develop and use a new method of analysis of nonadiabatic [i.e., when condition (1) is not satisfied near the tip of the rod] plasmon nanofocusing in rods with arbitrary taper angles, which is a combination of the rigorous finite-element analysis based on the commercially available software package COMSOL and adiabatic approximation. The rigorous analysis will be used close to the tip of the rod where condition (1) is not satisfied, while the adiabatic approximation will be used sufficiently far away from the tip where condition (1) is satisfied. Such a combination is useful, because using rigorous numerical methods in long tapered rods (of ~ 10 μm, which is the typical length of the optimized nanofocusing structures—see below) is highly inefficient and will require substantial computational resources.

It can be seen from Fig. 1(b) that at the vacuum wavelength $\lambda_{vac} = 632.8$ nm (He–Ne laser), for a gold tapered rod in vacuum [$\varepsilon_m = -11.44 + 1.12i$ (Ref. 23) and $\varepsilon_d = 1$] with taper angles as large as $\alpha = 90°$, the adiabatic approximation is valid for local rod diameters $2r \gtrsim 600$ nm (r is the local radius of the rod). For example, for all taper angles represented by the curves in Fig. 1(b), the left-hand side of inequality (1) is below ~ 0.01, if $r \gtrsim 300$ nm. Thus the adiabatic approximation is very well satisfied for rod radii $r \gtrsim 300$ nm. Therefore, we can use the rigorous finite-element analysis for $r < 300$ nm and adiabatic theory for $r > 300$ nm. The results obtained from both the approaches can then be matched at $r \approx 300$ nm, i.e., the amplitude of the plasmon incident onto the tip in the numerical approach is made equal to the amplitude of the plasmon obtained from the adiabatic theory.

In the numerical part of the analysis, we consider a section of the tapered rod between the initial radius $r = r_1 = 300$ nm and the rounded tip [Fig. 1(a)]. However, as we will see below, for larger taper angles ($\alpha \gtrsim 30°$) it is more convenient to extend the section of the tapered rod where the
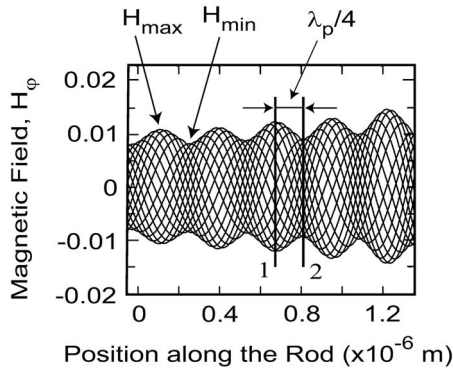
FIG. 2. Typical interference (standing wave) pattern formed by the incident (propagating toward the rounded tip) and reflected (propagating away from the rounded tip) plasmons in a tapered gold nanorod with taper angle α =6° and the radius of curvature of the tip $R=5$ nm at the vacuum wavelength $\lambda_{vac}=632.8$ nm (He–Ne laser); $\varepsilon_d=1$. Different curves correspond to the distribution of the magnetic field in the interfering plasmons at different initial phases of the launching field (between 0 and 2π), or, equivalently, at different moments of time during the evolution of the standing wave pattern within one period of the wave. H_{min} and H_{max} denote the neighboring maximum and minimum of the envelope curve, and λ_p is the local plasmon wavelength. Zero on the horizontal axis corresponds to ≈ 3 μm distance from the rounded tip.

rigorous numerical method is used to the initial rod radius $r_1=600$ nm. The plasmon is launched in this section of the rod by means of the boundary condition in COMSOL, specifying the magnetic field at the cross section of the rod at the radius $r=r_1$. The distribution of the launching magnetic field is assumed to equal to what it should be in the TM plasmon mode in a uniform rod with the radius $r=r_1=300$ nm (or 600 nm for $\alpha \geq 30°$). The numerical analysis using COMSOL has demonstrated that despite this chosen distribution of the launching magnetic field, the expected field distribution in the plasmon is achieved within a small distance from the launching point that is approximately equal to one plasmon wavelength. This is related to the Fabry–Perot resonance (multiple plasmon reflections between the point of the end-fire excitation and rounded tip) in the considered section of the tapered rod, while the launching boundary conditions are artificially fixed.

COMSOL provides an instantaneous field distribution in the section of the tapered rod between the point of the end-fire excitation with the local rod radius $r=r_1$ and the rounded tip. This instantaneous field distribution at every point corresponds to a standing wave pattern formed by the incident plasmon (propagating toward the tip of the rod) and reflected plasmon (propagating away from the tip). Changing phase of the launching field between 0 and 2π, we obtain time evolution of the standing wave pattern at every point of the tapered rod between the initial point with the radius $r=r_1$ and the rounded tip (Fig. 2). This pattern allows determination of the local amplitudes of the incident and reflected plasmons at a given distance from the rounded tip. Indeed, if two counterpropagating waves interfere with each other and their amplitudes are different, they will form a typical standing wave pattern shown in Fig. 2. The amplitudes of the incident and reflected waves can then be determined from the following simple equations:

$$H_{max} = H_i + H_r, \quad H_{min} = H_i - H_r, \tag{2}$$

where H_{min} and H_{max} denote numerically determined neighboring local minimum and maximum of the envelope curve for the standing wave pattern (Fig. 2), and H_i and H_r are the local amplitudes of the incident and reflected plasmons.

Note that this simple approach for the determination of the local amplitudes of the incident and reflected plasmons in a tapered section of a metal rod is only applicable if these amplitudes do not change significantly within one plasmon wavelength λ_p. This means that the difference between the values of H_{max} corresponding to two neighboring maxima of the envelope curve must be small compared to H_{max} at either of these maxima (Fig. 2). If this is not the case, i.e., the amplitudes of the incident and reflected plasmons change rapidly due to dissipation and/or nanofocusing effects on the rod, then the proposed method may lead to significant errors (this may be the case in the vicinity of the rounded tip, or when the taper angle is relatively large, i.e., $\gtrsim 30°$). To reduce these errors, Eq. (2) could be modified to incorporate varying plasmon amplitudes along the rod.

Typically, in good metals, dissipation is sufficiently weak, so that the plasmon propagates at least several wavelengths, which means that the variation of its amplitude within one plasmon wavelength (especially at relatively large rod diameters) is small. Therefore, dissipation-related variations of the plasmon amplitude within $\sim \lambda_p/4$ (Fig. 2) can be neglected. Only variations of the plasmon amplitude due to focusing effects could be noticeable at relatively large taper angles. In this case, Eq. (2) takes the form

$$H_{max} = H_{i1} + H_{r1}, \quad H_{min} = H_{i2} - H_{r2}, \tag{3}$$

where H_{i1}, H_{r1} and H_{i2}, H_{r2} are the amplitudes of the incident and reflected plasmons at the cross-sections 1 and 2, respectively, chosen at a maximum and the neighboring minimum of the envelope curve (Fig. 2).

Equation (3) cannot yet be used to determine the plasmon amplitudes, because they contain four unknown amplitudes. However, these amplitudes are not independent, and H_{i2} and H_{r2} can be expressed in terms of H_{i1} and H_{r1}. To do this, we write

$$H_{i2} = H_{i1} + \Delta H_{if}, \quad H_{r2} = H_{r1} + \Delta H_{rf}, \tag{4}$$

where the variations ΔH_{if} and ΔH_{rf} are caused by focusing effect on the tapered rod (dissipation-related variations are neglected). To calculate these variations, we note that the circumference of the rod cross-section 2 is smaller than the circumference of cross-section 1, because cross-section 2 is closer to the tip of the tapered rod by $\lambda_p/4$ (Fig. 2). The difference between the circumferences C_2 and C_1 of the rod cross-sections 2 and 1, respectively, is

$$\Delta C \equiv C_2 - C_1 = -0.5\pi\lambda_p \tan(\alpha/2). \tag{5}$$

Because $C_2 < C_1$, the energy flux in, for example, incident plasmon, which is proportional to $H_{i1}^2 C_1$ at cross-section 1, must now be spread over the smaller circumference of cross-section 2. Therefore, if the effect of dissipation within the distance of $\lambda_p/4$ is negligible, energy conservation requires that

$$H_{i1}^2 C_1 = (H_{i1} + \Delta H_{if})^2 (C_1 + \Delta C).$$

Here, we also assume that the coefficients of proportionality between the energy flux in the plasmon and $H^2 C$ are approximately the same for both cross-sections 1 and 2, and this is correct if these cross sections are sufficiently far from the tip, so that the variations of the plasmon wave number within one wavelength are negligible. This is equivalent to the adiabatic condition (1). At the same time, in the developed approach, the length of the rod section where we use rigorous numerical method must always be such that the adiabatic condition (1) is satisfied near the point of the end-fire excitation (in order to be able to match the adiabatic and nonadiabatic approaches). Retaining only the first order terms in ΔH_{if} and ΔC, and using Eq. (5) we obtain

$$\Delta H_{if} = \frac{\pi H_{i1} \lambda_p \tan(\alpha/2)}{4 C_1}. \tag{6}$$

Similarly, for the reflected plasmon,

$$\Delta H_{rf} = \frac{\pi H_{r1} \lambda_p \tan(\alpha/2)}{4 C_1}. \tag{7}$$

Substituting Eqs. (6) and (7) into Eq. (4) and then into Eq. (3) gives

$$H_{max} = H_{i1} + H_{r1},$$
$$H_{min} = (H_{i1} - H_{r1})\left(1 + \frac{\pi \lambda_p \tan(\alpha/2)}{4 C_1}\right), \tag{8}$$

where H_{min} is the first minimum of the envelope curve from the maximum H_{max} in the direction toward the tip of the rod (Fig. 2).

Equation (8) represents the next approximation for the determination of the local amplitudes H_{i1} and H_{r1} of the incident and reflected plasmons at a distance from the tip, corresponding to one of the maxima of the envelope curve (e.g., cross-section 1 in Fig. 2). Equation (8) is different from Eq. (2) by the presence of the second bracket in the right-hand side of the second of Eq. (8), which represents the correction due to variations of the plasmon amplitude caused by the focusing effects on the tapered rod. If necessary, the dissipation-related variation of the plasmon amplitude could also be taken into account in the same fashion.

Note that increasing the taper angle at a fixed initial radius of the rod $r = r_1$ results in a decrease in rod length. As a result, we have fewer maxima for the determination of the incident plasmon amplitude and increased rate of changing plasmon amplitude. This causes larger errors when using Eq. (8) for the determination of the incident plasmon amplitude. This is the reason why we use a larger initial radius $r_1 = 600$ nm for the section of the tapered rod where rigorous numerical analysis is conducted, if $\alpha \geq 30°$.

As indicated above, plasmon propagation in the tapered rod at local radii greater than $r_1 = 300$ nm (or 600 nm for $\alpha \geq 30°$) is considered using the adiabatic approximation.[12,13] We assume that the plasmon amplitude is known at some distance L from the tip (where the local rod diameter $r_0 > r_1$). Using the adiabatic approximation,[12,13] we determine
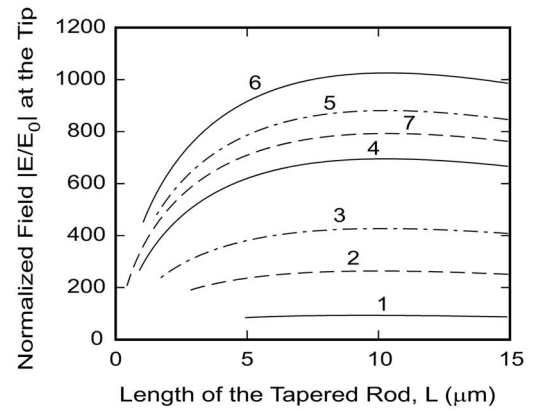

FIG. 3. The dependencies of the local electric field enhancement at the rounded (with the radius of curvature $R = 3$ nm) tip of the gold tapered rod on the length of this rod L; $\lambda_{vac} = 632.8$ nm (He–Ne laser), $\varepsilon_m = -11.44 + 1.12i$ (Ref. 23), and $\varepsilon_d = 1$ (the rod is surrounded by vacuum). The local electric field $|E|$ at the tip (i.e., at $z = 0$) is normalized to the amplitude of electric field $|E_0|$ in the plasmon at the initial cross section of the rod at $z = L$. This is equivalent to having $|E_0| = 1$ at $z = L$ (where $r = r_0$). Different curves correspond to different taper angles: (1) $\alpha = 6°$, (2) $\alpha = 10°$, (3) $\alpha = 14°$, (4) $\alpha = 20°$, (5) $\alpha = 30°$, (6) $\alpha = 36°$, and (7) $\alpha = 52°$.

the amplitude of the plasmon at the same distance from the tip where we have already found the amplitude of the incident plasmon in the rigorous numerical approach [i.e., by solving Eq. (8)]. This is typically about one plasmon wavelength from the point of the end-fire excitation toward the tip [where the standing wave pattern is established and the above-described method based on Eq. (2) or Eq. (8) can be used]. Then the plasmon field obtained in the numerical method at every point of the tapered rod where $r < r_1$ is divided by the amplitude of the incident plasmon determined in the numerical method at $r \approx r_1$ [i.e., from Eq. (8)], and multiplied by the same amplitude obtained at the same point in the adiabatic theory. Thus we match the plasmon field from the approximate adiabatic theory used for the description of plasmon propagation at $r \gtrsim r_1$ with the plasmon field from the rigorous finite-element analysis used for the description of plasmon propagation near the tip (at $r < r_1$). This approach allows the efficient analysis of plasmon propagation in long tapered rods (up to tens of micron length) and enables optimization of these nanofocusing structures.

III. RESULTS AND DISCUSSIONS

Figure 3 shows the dependencies of the local electric field enhancement at the rounded tip (with the radius of curvature $R = 3$ nm) of the gold tapered rod on the length of the rod, i.e., distance at which the amplitude of the incident plasmon is assumed to equal to 1. Several important aspects can be seen from this figure.

First, increasing the taper angle initially results in an increase in the local field enhancement at the rounded tip for all considered lengths of the rod (compare curves 1–6 in Fig. 3). At an optimal angle, the local field enhancement reaches a maximum (curve 6) and then starts decreasing for all considered lengths of the rod, when the taper angle is increased further (compare curves 6 and 7). Note that the existence of an optimal taper angle for nanofocusing in tapered rods and

gaps has been investigated earlier in Refs. 14, 17, and 20. The existence of an optimal angle of a tapered rod is related to the competition of the following two opposing mechanisms associated with plasmon propagation in such structures.

Suppose that the length L of the tapered rod is fixed, but the taper angle α could be changed. Then, increasing α results in an increase in the circumference of the initial cross section of the tapered rod at $z=L$. Therefore, if the amplitude of the incident plasmon at the initial cross section $z=L$ is $|E_0|=1$ for all taper angles, then the energy in the incident plasmon at the initial cross section will increase with increasing taper angle. This must lead to a tendency of increasing local field enhancement at the tip with increasing α, because larger energy of the incident plasmon will have to be focused into the same nanoregion that is of the order of the radius of curvature of the rounded tip. On the other hand, significantly increasing the taper angle results in enhanced breaching in the adiabatic approximation near the tip [Fig. 1(b)], and this will lead to significant reflections of the plasmon from the taper near the tip. As a result, a significant portion of the energy of the incident plasmon will be reflected back from the taper before it is able to reach the tip of the rod. This effect increases with increasing taper angle, resulting in a tendency of decreasing local field at the tip. Competition of these two opposing mechanisms results in an optimal taper angle at which the local field enhancement at the tip is maximal (see Figs. 3 and 4).

The second important feature that can be seen from Fig. 3 is that increasing the length L of the tapered gold rod initially results in an increase in the local field enhancement (this is the confirmation of the similar finding made earlier by Issa and Guckenberger[14]). However, at $L=L_{opt} \sim 10$ μm, the local field enhancement at the rounded tip reaches a maximum, and further increase in rod length results in a monotonic decrease in the field enhancement at the tip (curves 2–7 in Fig. 3). This can again be understood by considering two opposing mechanisms for variations of the plasmon amplitude in the rod. One of these mechanisms is related to focusing effects on the tapered metal rod [see the derivation of Eqs. (3)–(7)] and to plasmon dissipation. If the plasmon propagates from a cross section of the rod with the coordinate z to the cross section with the coordinate $(z-dz)$ (closer to the tip), then its amplitude tends to increase because the plasmon energy must now be spread over the smaller circumference of the cross section at $z-dz$ [see also Eqs. (4)–(7)]. This effect occurs at all distances from the tip of the tapered rod. However, increasing the distance from the tip results in a decrease in the relative variations of the circumference for a fixed value of dz. This means that at large distances from the tip of the tapered rod, increase in the plasmon amplitude as it propagates the distance dz toward the tip can be arbitrarily small (tending to zero with increasing distance from the tip to infinity). On the other hand, at similar large distances from the tip, the rate of dissipation of the plasmon in the rod tends to a finite value corresponding to the dissipation rate of the plasmon on a flat metal surface. Therefore, at large distances from the tip, dissipation should be the dominant mechanism resulting in reduction of the
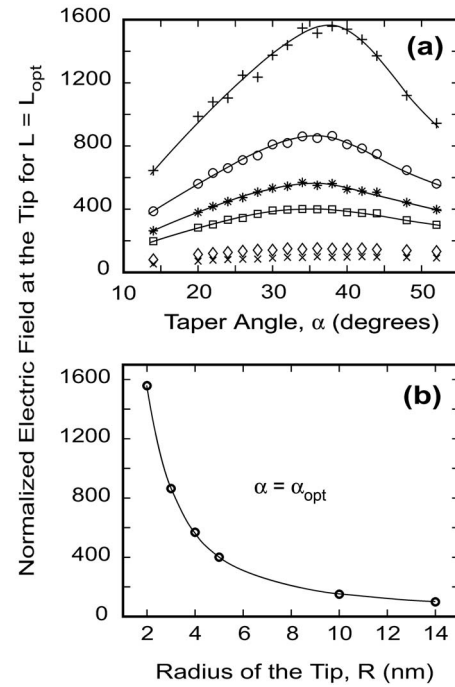

FIG. 4. Demonstration of the effect of different radii of curvature on the rounded tip of the gold tapered rod of optimal length $L=L_{opt}$ in vacuum: $\varepsilon_m=-11.44+1.12i$ (Ref. 23), $\varepsilon_d=1$, and $\lambda_{vac}=632.8$ nm (He–Ne laser). (a) The dependencies of the local electric field enhancement at the tip of the tapered gold rod on the taper angle at optimal rod length and different radii of curvature of the tip: (+) $R=2$ nm; ($\bigcirc$) $R=3$ nm; ($\ast$) $R=4$ nm; ($\square$) $R=5$ nm; ($\diamond$) $R=10$ nm; ($\times$) $R=14$ nm. (b) The dependence of the maximal possible local electric field enhancement at the rounded tip of the rod (i.e., at the optimal length of the rod and optimal taper angle) on the radius of curvature R of the tip. The normalization of the local electric field $|E|$ at the tip (i.e., at $z=0$) is conducted to the initial amplitude of electric field $|E_0|$ in the plasmon at $z=L$.

plasmon amplitude as it propagates toward the tip, whereas at small distances focusing effects become dominant, resulting in increasing plasmon amplitude as it propagates toward the tip. It follows from here that there is a distance from the tip at which dissipation and the focusing effects exactly cancel each other. This distance is equal to the optimal length of the tapered rod L_{opt}, at which local field enhancement at the tip is maximal.

It is easy to derive an approximate analytical equation for the optimal length of a tapered metal rod. If dissipation is sufficiently weak, mutual cancellation of the dissipation and focusing effects occurs at a large distance from the tip of the rod, where the local rod radius is large compared to the plasmon wavelength. In this case, dissipation rate is determined using the approximation that the plasmon propagates along a flat metal interface. Thus we determine the dissipation-related variation of the plasmon amplitude as the plasmon propagates from the cross-section z to the cross-section $z-dz$. Then, assuming that dissipation is zero, and calculating the difference between the circumferences of the cross-sections z and $z-dz$, we use energy conservation to determine the variation (increment) in the plasmon amplitude caused by the focusing effect [similarly to how it was done for Eqs. (4)–(7)]. At the optimal distance from the tip of the rod, the sum of these two variations of the plasmon ampli-

tude must be equal to zero. This gives us the following equation for the optimal length of the tapered rod:

$$L_{opt} \approx \frac{e_1(\varepsilon_d + e_1)}{e_2 \varepsilon_d q_0} \cos(\alpha/2), \tag{9}$$

where q_0 is the real part of the wave number of the surface plasmon on the flat metal interface (i.e., when $r = +\infty$).

As mentioned above, Eq. (9) is approximately correct if the local rod diameter at $z = L_{opt}$ is significantly larger than the plasmon wavelength. It is easy to see that this condition is satisfied if

$$\sin(\alpha/2) \gg \frac{e_2 \varepsilon_d}{e_1(\varepsilon_d + e_1)}. \tag{10}$$

It is important that Eq. (9) provides an extremely simple analytical equation for the required metal rod parameters in order to ensure maximal local field enhancement at the tip. Note that this equation [as well as its applicability condition (10)] does not depend on the radius of curvature of the rounded tip. However, it depends on frequency, because q_0 and the real and imaginary parts of the metal permittivity are frequency dependent.

For example, for a gold tapered rod in vacuum and at vacuum wavelength $\lambda_{vac} = 632.8$ nm, applicability condition (10) suggests that Eq. (9) should be approximately correct for taper angles $\alpha > 10°$, and the optimal rod length is ~ 10 μm within the range $10° < \alpha < 80°$. It is interesting that optimal rod length only weakly depends on the taper angle of the rod. This finding is in good agreement with Fig. 3, which also demonstrates that the maximum of the local field enhancement at the tip is achieved at the rod length ~ 10 μm for all considered taper angles above 10° (see curves 2–7 in Fig. 3).

Similarly, for a silver tapered rod in vacuum and at the vacuum wavelength $\lambda_{vaac} = 632.8$ nm, applicability condition (10) gives taper angles $\alpha > 4°$, and within the range $4° < \alpha < 80°$, the optimal length of the rod is ~ 20 μm.

Note also that typically there is no need to determine the optimal rod length very accurately, because the maximum of the local field enhancement as a function of rod length is typically broad. For example, as can be seen from Fig. 3, variations of the gold rod length between ~ 5 and ~ 15 μm do not have a profound effect on the achievable local field enhancement at the tip. This is beneficial from the practical point view, because it demonstrates high tolerance of the described nanofocusing structures (tapered metal rods) to structural imperfections and fabrication uncertainties. Therefore, Eq. (9) should be regarded as an excellent guide for the reliable determination of the optimal structural parameters in a wide range of taper angles.

It is important to note that the optimal lengths of the tapered metal rod have been determined by means of excluding multiple reflections from the point of the end-fire excitation (see Sec. II). Certainly, if such multiple reflections (the Fabry–Perot effect) exist in the struckure, they may have a significant impact on nanofocusing and, in particular, optimal length of the rod. Equations (9) and (10) were derived in the absence of reflections from the point of the end-fire excita-

tion. At the same time, taking such reflections into account in the current model would be inappropriate, because they would have been related to a nonphysical boundary condition at the point of the end-fire excitation, where the plasmon field was artificially fixed (see Sec. II). This is not what typically happens in a physically realistic situation, for example, when the tapered metal rod is attached to an optical fiber. Therefore, the Fabry–Perot effect in the tapered section of the rod has been eliminated by means of the discussed normalization of the obtained local field enhancement and matching the incident wave amplitude near the point of the end-fire excitation to that obtained from the adiabatic theory (see Sec. II). The question about a realistic Fabry–Perot effect in a section of a tapered rod with the subsequent optimization of the structural parameters is a separate problem that is beyond the scope of the current paper.

There are two other important aspects that can further be drawn from Fig. 3. First, even in the gold nanorods, achieving very strong local field enhancement does not seem to be a problem (in silver rods the enhancement is even greater). For example, local field enhancement at the tip of the radius of curvature $R = 3$ nm at the optimal taper angle and optimal rod length (curve 6) is such that it should provide an ~ 12 order enhancement of the Raman signal, which is close to what is required for single molecule detection. Second, typical optimal lengths of the nanofocusing rods are in micrometers, which is a significant simplification for fabrication and practical use of these structures, for example, as tips in scanning near-field microscopy and spectroscopy.

The effect of curvature of the rounded tip on the local field enhancement is demonstrated in Fig. 4. For example, as can be seen from Fig. 4(a), local field enhancement at the tip rapidly increases with decreasing radius of curvature R of the tip. Varying R from 5 to 2 nm results in an approximately four times increase in the local electric field enhancement, demonstrating high sensitivity of the rod structure to the radius of the tip. Therefore, careful fabrication of the rounded tip of the tapered rod is crucial for achieving required controllable local field enhancement. On the other hand, the optimal taper angle hardly depends on R [compare the curves in Fig. 4(a)]. It is possible to notice only very weak tendency toward increasing optimal taper angle with decreasing radius of the tip. As has been indicated above, optimal rod length is also independent of R.

Figure 4(b) presents the dependence of the absolute maximum of the local electric field enhancement at the rounded tip [at the optimal taper angle and optimal length of the rod—see the maxima on the curves in Fig. 4(a)] on the radius of curvature of the tip. Further reduction of the tip radius R is unreasonable, because this would require consideration of spatial dispersion, Landau damping, and atomic structure of matter[12] (which is beyond the scope of this paper). The radius of the tip of ~ 2 nm can thus be regarded as the lower limit for the reasonable applicability of the developed theory of nanofocusing in tapered metal rods, which is based on the approximation of continuous electrodynamics.
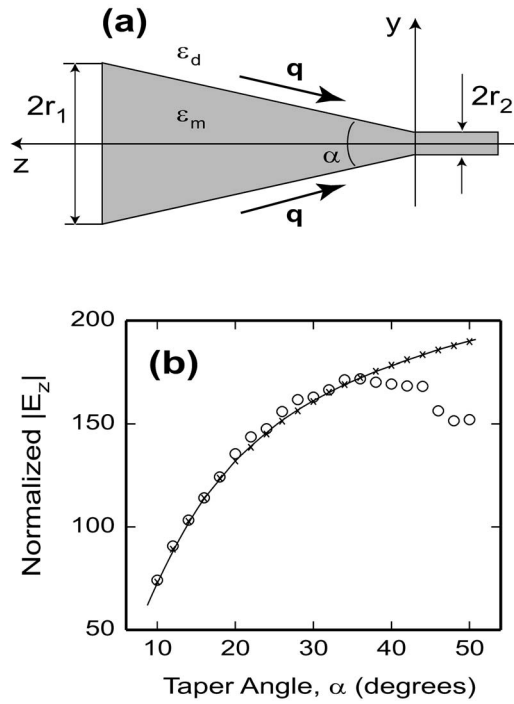
FIG. 5. (a) The structure used for the comparison of the adiabatic and nonadiabatic theories of nanofocusing in a tapered metal rod. A uniform metal nanowire of the same material as the tapered rod is attached to the smallest (exit) cross section of the rod in order to suppress (reduce) plasmon reflections from the tip. (b) The dependencies of the z-component of the electric field in the focused TM plasmon in the vacuum near the metal surface at the smallest (exit) cross section of radius $r=r_2$ of the tapered section of the gold rod on the taper angle α; $\lambda_{vac}=632.8$ nm, $\varepsilon_m=-11.44 +1.12i$ (Ref. 23), $\varepsilon_d=1$, $r_1=300$ nm, and $r_2=5$ nm. The crosses and solid curve represent the results from the adiabatic theory (Refs. 12 and 13). The circles represent the results from the nonadiabatic rigorous theory based on finite-element analysis.

IV. ADIABATIC VERSUS NONADIABATIC THEORY

In this section, we compare the adiabatic and nonadiabatic theories of nanofocusing in tapered metal rods and, in particular, determine/verify numerically the applicability conditions for the adiabatic theory.[12,13] Adiabatic theory assumes no plasmon reflections from the tip of the rod.[12,13] At the same time, numerical analysis of nanofocusing in tapered rods with rounded tips always results in some plasmon reflection from the tip. The reflected plasmon inevitably contributes to the overall local field in the rod (see Sec. II). Therefore, in order to sensibly compare the approximate (adiabatic) and rigorous numerical results, we need to eliminate reflections from the tip in the numerical approach. This could be achieved by means of attaching a uniform nanowire to the exit cross section of the tapered rod, such that the diameter of the nanowire is equal to the smallest (exit) diameter of the tapered rod [Fig. 5(a)].

The length of the nanowire is chosen to ensure efficient dissipation of the plasmon, i.e., suppressing plasmon reflections from the free end of the nanowire. In this case, the plasmon will largely continue propagating into the wire, rather than being reflected from the exit section of the tapered section of the rod (if the angle α is not too large). Thus there will be no reflected plasmon in the tapered section of the rod, which enables the direct comparison with the adiabatic theory of nanofocusing.[12,13]

As an example, the comparison between the adiabatic and nonadiabatic theories of nanofocusing is conducted for a gold tapered rod with the gold nanowire attached to it [Fig. 5(a)]. The resultant dependencies of the z-component of the electric field near the surface of the rod at $z=0$, i.e., at the exit cross section [Fig. 5(a)], on the taper angle α are shown in Fig. 5(b) for the adiabatic theory (crosses and solid curve) and nonadiabatic rigorous numerical analysis (circles). The other structural parameters are shown in the figure caption for Fig. 5.

It can be seen that the adiabatic theory is approximately valid up to $\sim 35°$ taper angle. Above these values of α, reflections of the plasmon from the taper itself appear to be strong enough to noticeably reduce the overall energy reaching the exit cross section at $z=0$ [Fig. 5(a)], and this results in decreasing local field enhancement at $z=0$ in the rigorous numerical analysis, compared to the adiabatic theory. This explains the significant deviation of the numerical curve from that obtained in the adiabatic approximation for larger taper angles $\alpha > 35°$ [Fig. 5(b)].

The fact that the adiabatic theory appears to be valid up to angles $\sim 35°$ is quite remarkable. These angles appear to be significantly larger than those for a tapered groove.[17,20] At this stage, physical explanation of this difference is not entirely clear, but it should be related to weaker reflections of the plasmon in a tapered rod compared to a tapered groove. This seems to be a noticeable advantage of a tapered rod as a nanofocusing structure. This is because tapered rods with larger taper angles are easier to fabricate, and increasing the taper angle results in a decrease in the contribution of the dissipative effects on the plasmon amplitude (decreasing dissipative energy losses), which opens a possibility for achieving significantly larger local field enhancements.

It is also interesting that condition (1) that has been highlighted as the applicability condition for the adiabatic theory seems to be too restrictive, and the approximate theory is actually applicable for significantly larger angles for which $d(Q_1^{-1})/dz$ could be of the order of 1. Therefore, the applicability condition (1) should rather be written in the form

$$\left| \frac{d(Q_1^{-1})}{dz} \right| \lesssim 1. \tag{1'}$$

For example, at $\alpha=35°$ and the local radius of the rod $r =5$ nm, the left-hand side in inequality (1) is ≈ 0.84. This demonstrates that the rate of changing wave number of the strongly localized plasmon in a tapered rod is smaller than for the tapered groove. This is because similar values of the left-hand side in inequality (1) for a tapered groove are obtained at significantly smaller taper angles.[17,20]

The values of the taper angles [$\sim 35°$ in Fig. 5(b)] at which the adiabatic approximation ceases to be applicable are approximately equal to the optimal angles for achieving the largest possible field enhancement at the rounded tip [Fig. 4(a)]. This is expected, because the largest local field enhancement is achieved when the taper angle is increased as much as possible (to reduce the effect of dissipative losses in the rod), but only up to the angle at which the reflections from the taper become significant, i.e., where the adiabatic approximation ceases to apply.

V. CONCLUSIONS

The results obtained in this paper have provided important practical information and criteria for fabrication and use of optimal nanofocusing structures based on plasmon propagation in tapered metal rods. In particular, we have confirmed the existence of optimal taper angle providing strong local electric field enhancement at the tip (which was previously suggested by Issa and Guckenberger[14]). We have demonstrated the existence of the optimal length of the tapered rod, which, in combination with the optimal taper angle, provides the maximal possible local field enhancement at the rounded tip of fixed radius of curvature. A simple analytical equation for the optimal rod length has been derived from basic physical principles and verified against the rigorous numerical results. Three order of magnitude local field enhancements are shown to be achievable during plasmon nanofocusing in gold and especially silver nanorods. Strong dependence of the local field enhancement on the radius of curvature of the tip has also been demonstrated and investigated.

One of the important practical outcomes of this paper is that the optimal nanofocusing structures using metal rods are relatively large. For example, the optimal length for a gold (silver) rod is ~ 10 μm (~ 20 μm), while the optimal taper angle for the gold rod is $\approx 36°$. This means that the initial diameter of the tapered nanofocusing rod should be ~ 6 μm, in order to achieve maximal possible field enhancement at the tip. Such optimal tapered rods should be relatively easy to fabricate. Due to their geometrical parameters and dimensions, they should be strong and durable in use. Light could be relatively easily coupled into plasmons propagating in such rods. Moreover, it has been demonstrated that variations of rod length around the optimal length by up to $\sim 50\%$ (e.g., between ~ 5 and 15 μm for the gold rod) do not result in significant variations of the resultant local field enhancement at the rounded tip. This demonstrates high tolerance of the described structures to fluctuations of rod length, and this seems to be highly beneficial for fabrication and practical use.

At the same time, it has been demonstrated that plasmon nanofocusing is highly sensitive to the conditions at the tip of the tapered rod and, in particular, to its radius of curvature. Therefore, one should pay significant attention to accurate fabrication of the actual tip, including its shape and dimensions. Proper fabrication of the rounded tip should ensure reproducible and strong local field enhancement of up to three orders of magnitude.

The comparison of the obtained numerical results with those from the adiabatic theory of nanofocusing has demonstrated the validity of the approximate theory in a relatively broad range of taper angles up to $\sim 35°$ (for gold rods),

which opens wider opportunities for the successful use of the adiabatic theory of nanofocusing in tapered metal rods.[12,13]

The obtained results will be important for the near-field microscopy and spectroscopy, optimal design of optical couplers for most effective delivery of the electromagnetic energy to nano-optical devices, quantum dots, single molecules, for the development of new optical sensors and measurement techniques (e.g., based on surface-enhanced Raman spectroscopy combined with nanofocusing), etc.

[1] D. W. Pohl, W. Denk, and M. Lanz, Appl. Phys. Lett. **44**, 651 (1984).
[2] L. Novotny and C. Hafner, Phys. Rev. E **50**, 4094 (1994).
[3] L. Novotny, D. W. Pohl, and B. Hecht, Ultramicroscopy **61**, 1 (1995).
[4] *Near-Field Optics and Surface Plasmon-Polaritons*, Topics in Applied Physics Vol. 81, edited by S. Kawata (Springer-Verlag, Berlin, 2001).
[5] A. Bouhelier, J. Renger, M. R. Beversluis, and L. Novotny, J. Microsc. **210**, 220 (2003).
[6] N. Anderson, A. Bouhelier, and L. Novotny, J. Opt. A, Pure Appl. Opt. **8**, S227 (2006).
[7] D. Mehtani, N. Lee, R. D. Hartschuh, A. Kisliuk, M. D. Foster, A. P. Sokolov, F. Cajko, and I. Tsukerman, J. Opt. A, Pure Appl. Opt. **8**, S183 (2006).
[8] K. V. Nerkararyan, T. Abrahamyan, E. Janunts, R. Khachatryan, and S. Harutyunyan, Phys. Lett. A **350**, 147 (2006).
[9] K. Li, M. I. Stockman, and D. J. Bergman, Phys. Rev. Lett. **91**, 227402 (2003).
[10] K. Li, M. I. Stockman, and D. J. Bergman, Phys. Rev. B **72**, 153401 (2005).
[11] A. J. Babadjanyan, N. L. Margaryan, and K. V. Nerkararyan, J. Appl. Phys. **87**, 3785 (2000).
[12] M. I. Stockman, Phys. Rev. Lett. **93**, 137404 (2004).
[13] M. W. Vogel and D. K. Gramotnev, Phys. Lett. A **363**, 507 (2007).
[14] N. A. Issa and R. Guckenberger, Plasmonics **2**, 31 (2007).
[15] N. A. Issa and R. Guckenberger, Opt. Express **15**, 12131 (2007).
[16] D. K. Gramotnev, J. Appl. Phys. **98**, 104302 (2005).
[17] D. F. P. Pile and D. K. Gramotnev, Appl. Phys. Lett. **89**, 041111 (2006).
[18] D. K. Gramotnev and K. C. Vernon, Appl. Phys. B: Lasers Opt. **86**, 7 (2007).
[19] P. Ginzburg, D. Arbel, and M. Orenstein, Opt. Lett. **31**, 3288 (2006).
[20] D. K. Gramotnev, D. F. P. Pile, M. W. Vogel, and X. Zhang, Phys. Rev. B **75**, 035431 (2007).
[21] K. C. Vernon, D. K. Gramotnev, and D. F. P. Pile, J. Appl. Phys. **101**, 104312 (2007).
[22] M. Durach, A. Rusina, M. I. Stockman, and K. Nelson, Nano Lett. **7**, 3145 (2007).
[23] E. D. Palik, *Handbook of Optical Constants of Solids* (Academic, New York, 1985).